Electronic supplementary information

Contact resistance based tactile sensor using covalently cross-linked graphene aerogels

*Prabhat Kumar, Martin Šilhavík, Zahid Ali Zafar and Jiří Červenka**

Department of Thin Films and Nanostructures, Institute of Physics of the Czech Academy of Sciences, Cukrovarnická 10/112, Prague - 162 00, Czech Republic
*Email: cervenka@fzu.cz

*Author to whom correspondence should be addressed. Email: cervenka@fzu.cz

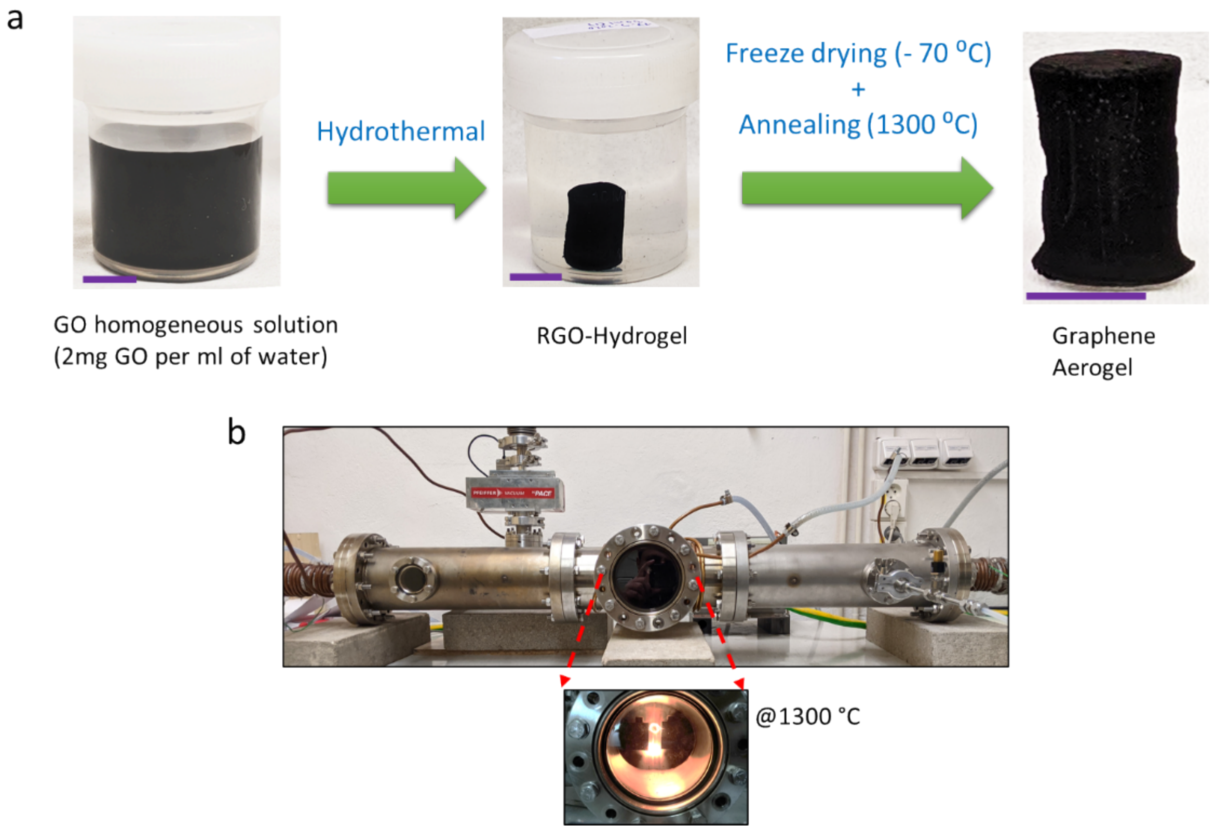

Figure S1: (a) Actual pictures of the materials obtained after every step of synthesizing 3D graphene aerogels (scale bar: 1 cm). (b) actual photograph of home-made high temperature vacuum furnace.

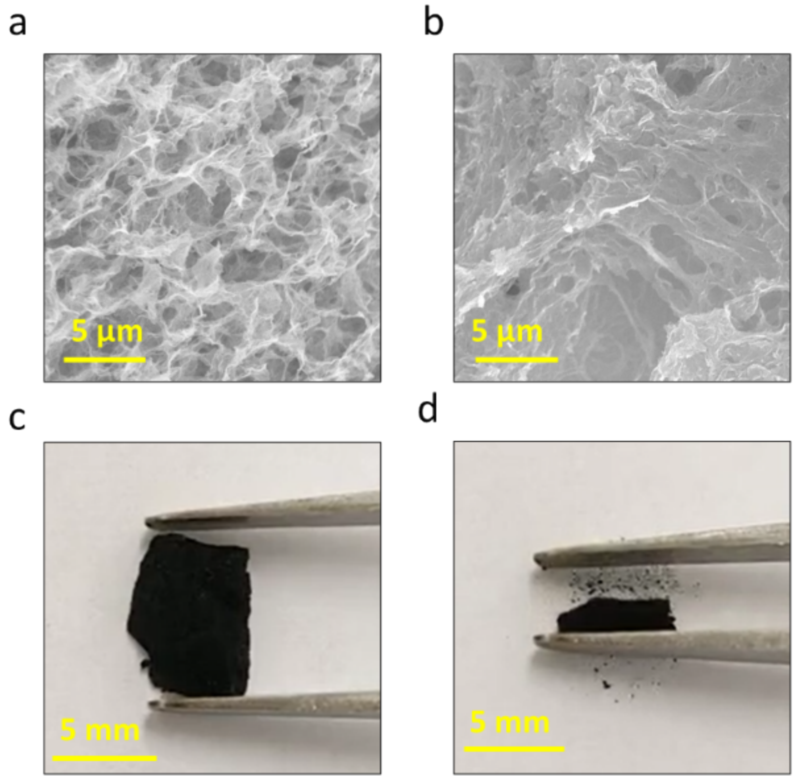

Figure S2: SEM micrograph of non-annealed graphene aerogel (a) uncompressed state, (b) compressed state, (c-d) actual photograph of non-annealed samples in uncompressed and compressed state.

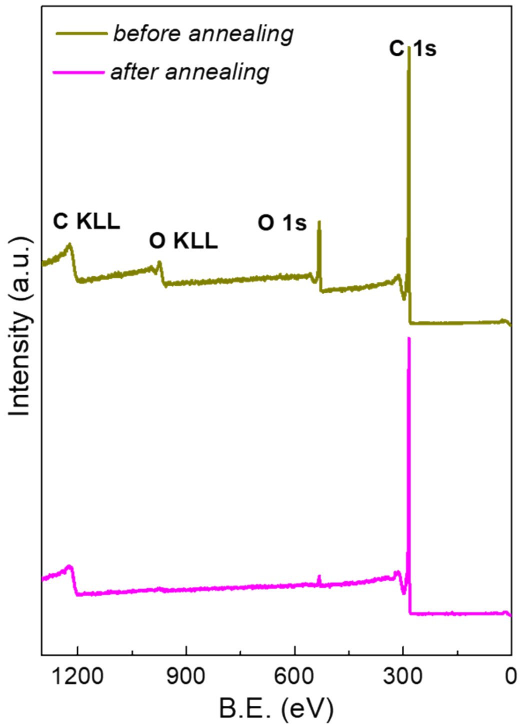

Figure S3: XPS survey scans of a 3D graphene aerogel before and after annealing.

Table S1: XPS compositional analysis of a 3D graphene aerogel before and after the annealing.

Sample	Etch (sec)	C (at.%)	O (at.%)
Before annealing GA	0	88.2	11.8
	30	88.7	11.3
After annealing GA	0	98.4	1.6
	30	98.3	1.7

Table S2: Deconvolution peak analysis of C 1s peaks in 3D graphene aerogel before and after annealing.

Sample	Peaks	C sp^2	C sp^3	C-O	O-C=O	π- π*
Before annealing GA	Position (eV)	284.4	285.0	286.0	288.5	291.5
	FWHM (eV)	0.7	0.9	1.6	3.3	5.6
	Area %	53.7	11.4	13.6	13.3	8
After annealing GA	Position (eV)	284.4	285.0	286.0	287.5	291.2
	FWHM (eV)	0.6	0.9	1.9	3.7	5.7
	Area %	70.5	8.9	6.1	6.1	8.4

Table S3: Deconvolution peak analysis of O 1s peak in 3D graphene aerogel before and after annealing.

Sample	Peaks	C-O	C=O	O-C=O
Before annealing GA	Position (eV)	533.1	531.7	530.7
	FWHM (eV)	1.8	1.8	1.8
	Area %	50.8	28	21.2
After annealing GA	Position (eV)	533.0	531.9	-
	FWHM (eV)	1.8	1.8	-
	Area %	63.4	36.6	-

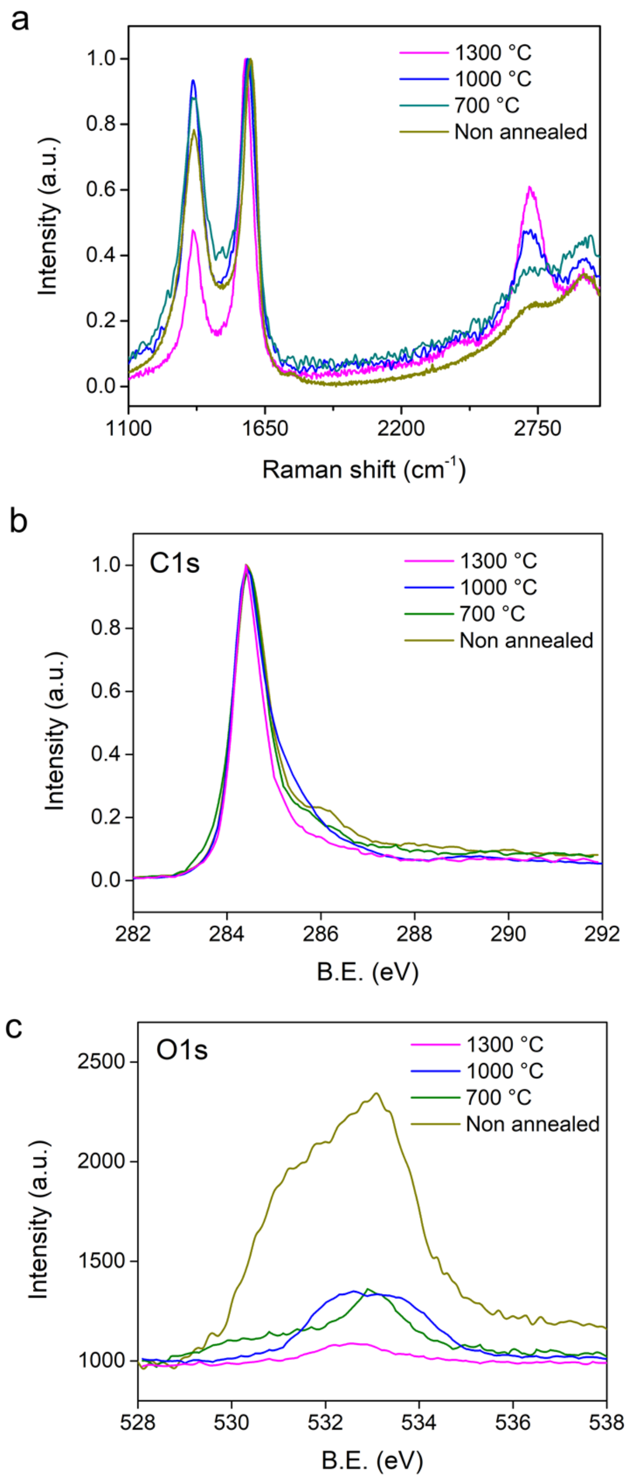

Figure S4: Raman spectroscopy and XPS analysis of graphene aerogels annealed at different temperatures in vacuum.

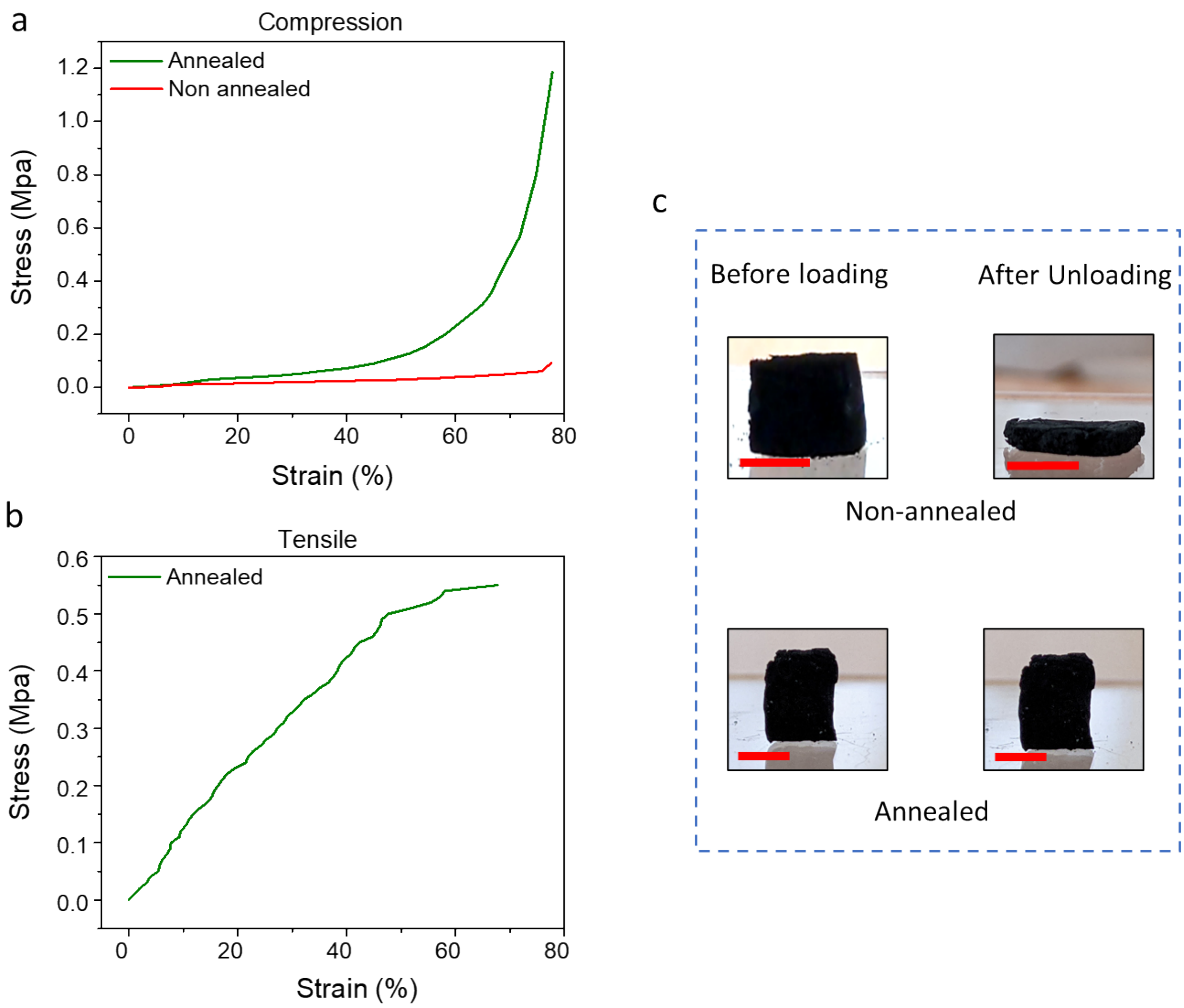

Figure S5: The stress-strain curve of graphene aerogel in (a) compression and (b) tensile. (c) actual photographs of non-annealead and annealead graphene aerogel before and after loading (scale bar: 5 mm).

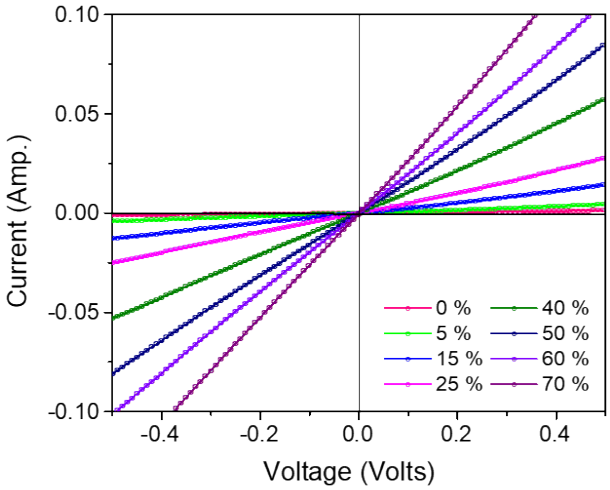

Figure S6: I-V measurements of a GA sensor under an increasing compressive strain demonstrating a linear relationship between current (I) and voltage (V). The slope of the I–V curves increases with increasing applied pressure.

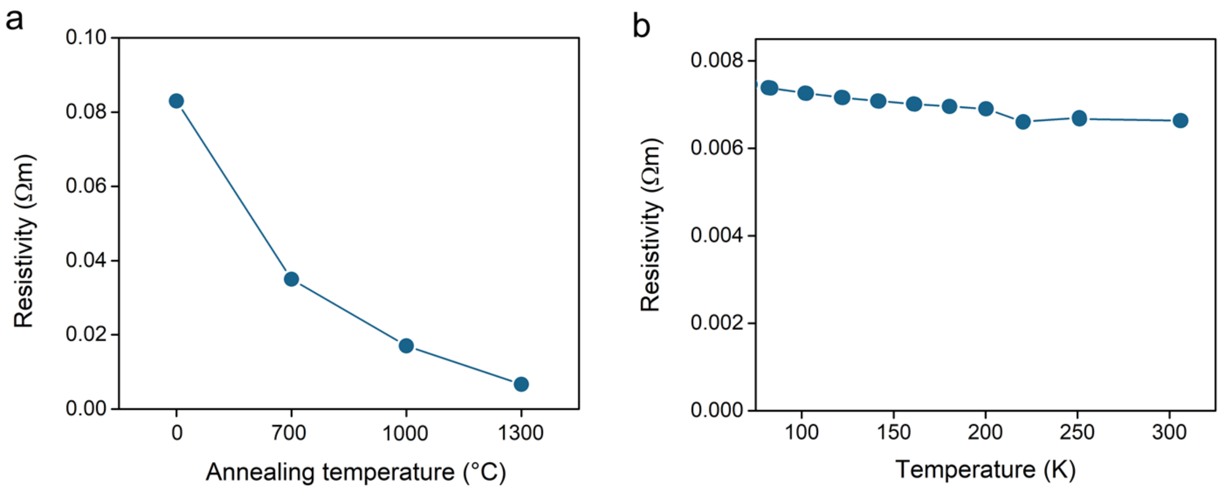

Figure S7: Resistivity of graphene aerogels as a function of (a) sample annealing temperature and (b) temperature. The temperature dependent resistivity was measured using a graphene aerogel sample annealed at 1300 °C. Resistivity of the samples was determined using the van der Pauw method in a 4-point probe geometry.

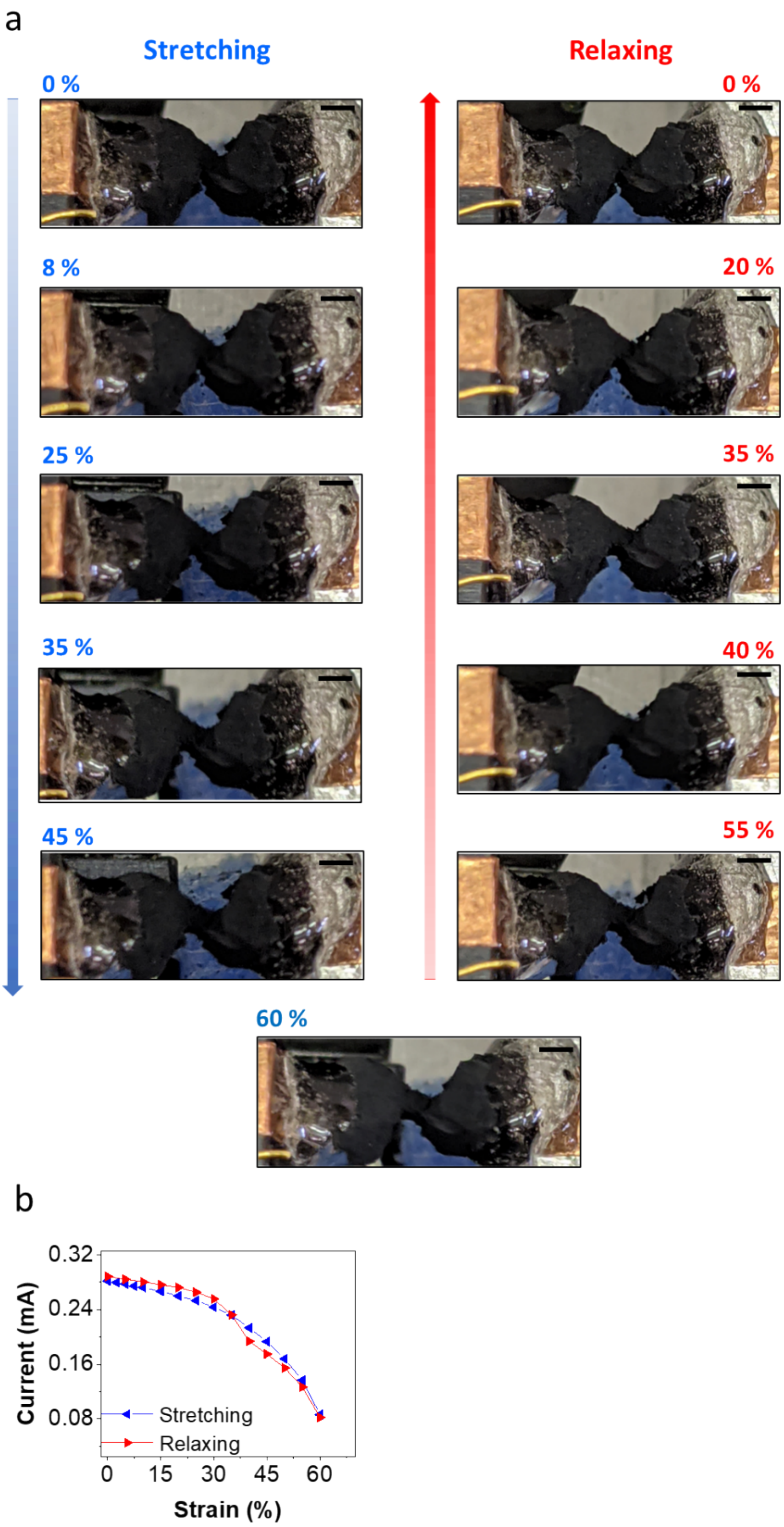

Figure S8: (a) Photographs showing reversible mechanical and electrical nature of GA under the tensile strain (scale bar: 3 mm) and (b) the corresponding current-strain response of the GA sensor.

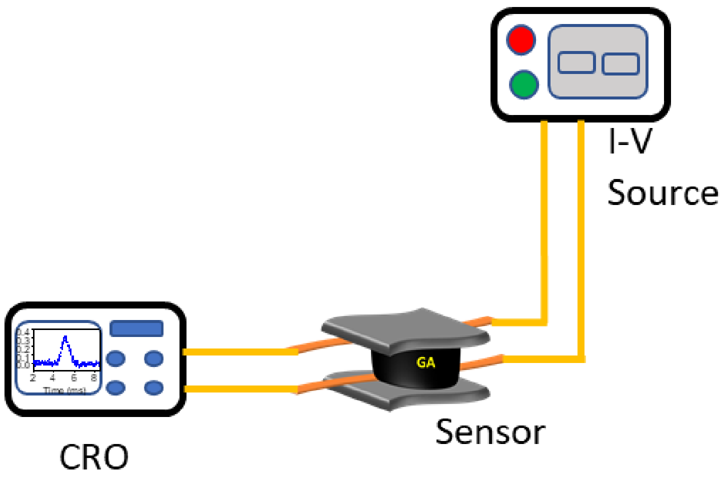

Figure S9: Schematics of the experimental configuration for measuring the fast dynamic voltage response of the sensors

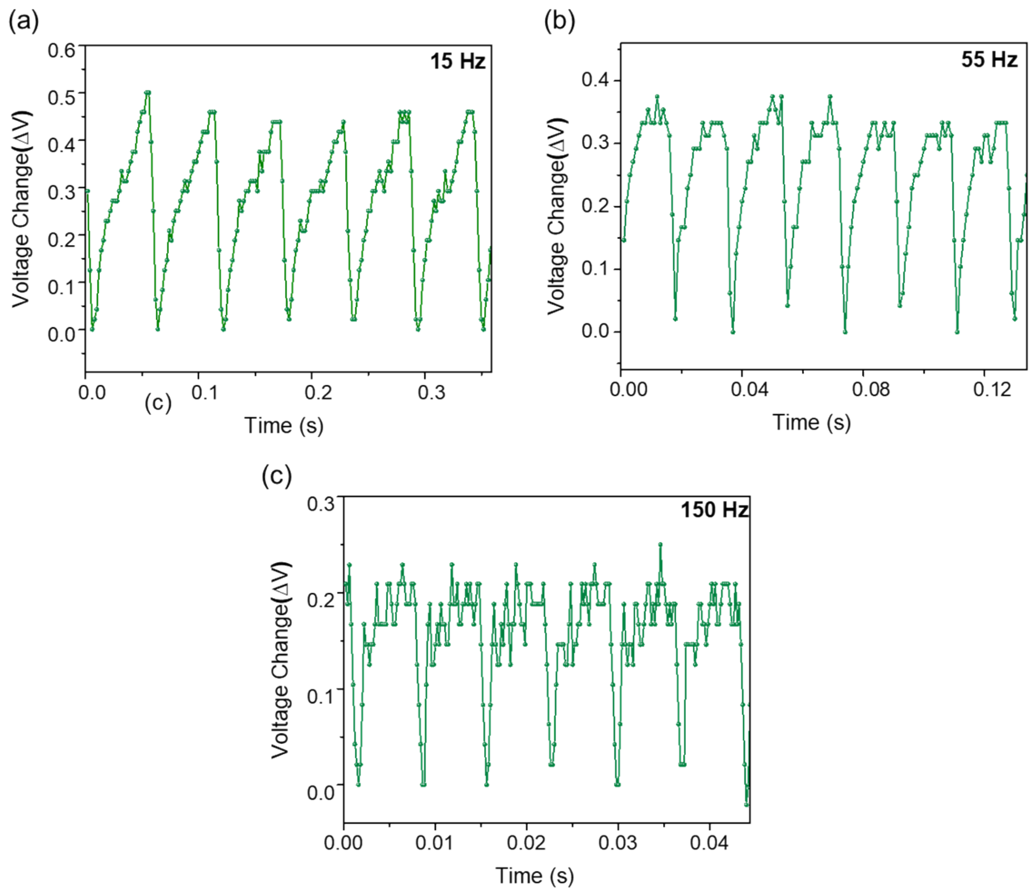

Figure S10: Dynamic response of a GA sensor at (a) 15 Hz (b) 55 Hz and (c) 150 Hz at repetitive 10% compressive strain pressure conditions using an external electric motor.

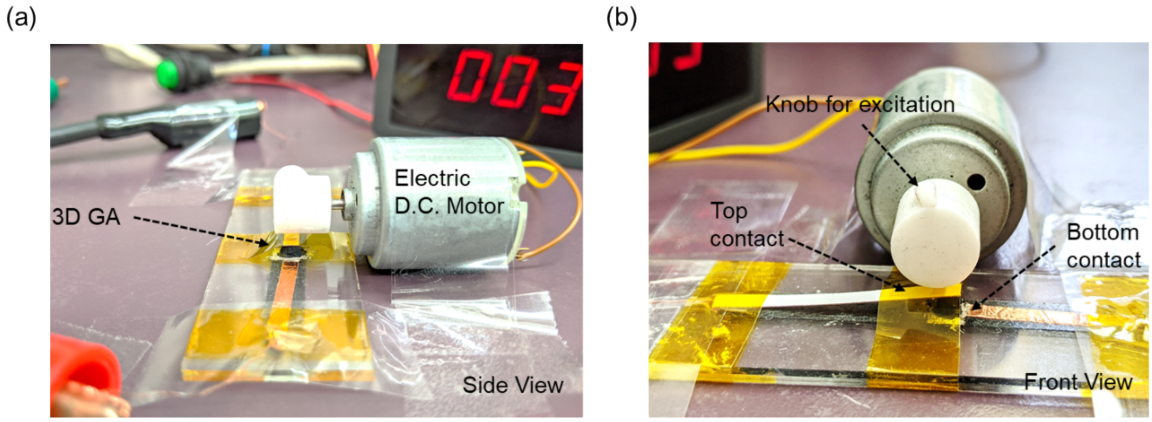

Figure S11: Experimental set-up to excite the sensor at different frequencies of 15-150 Hz using an external electric motor showing (a) side view and (b) front view. The frequency is changed by varying the applied voltage across the motor.

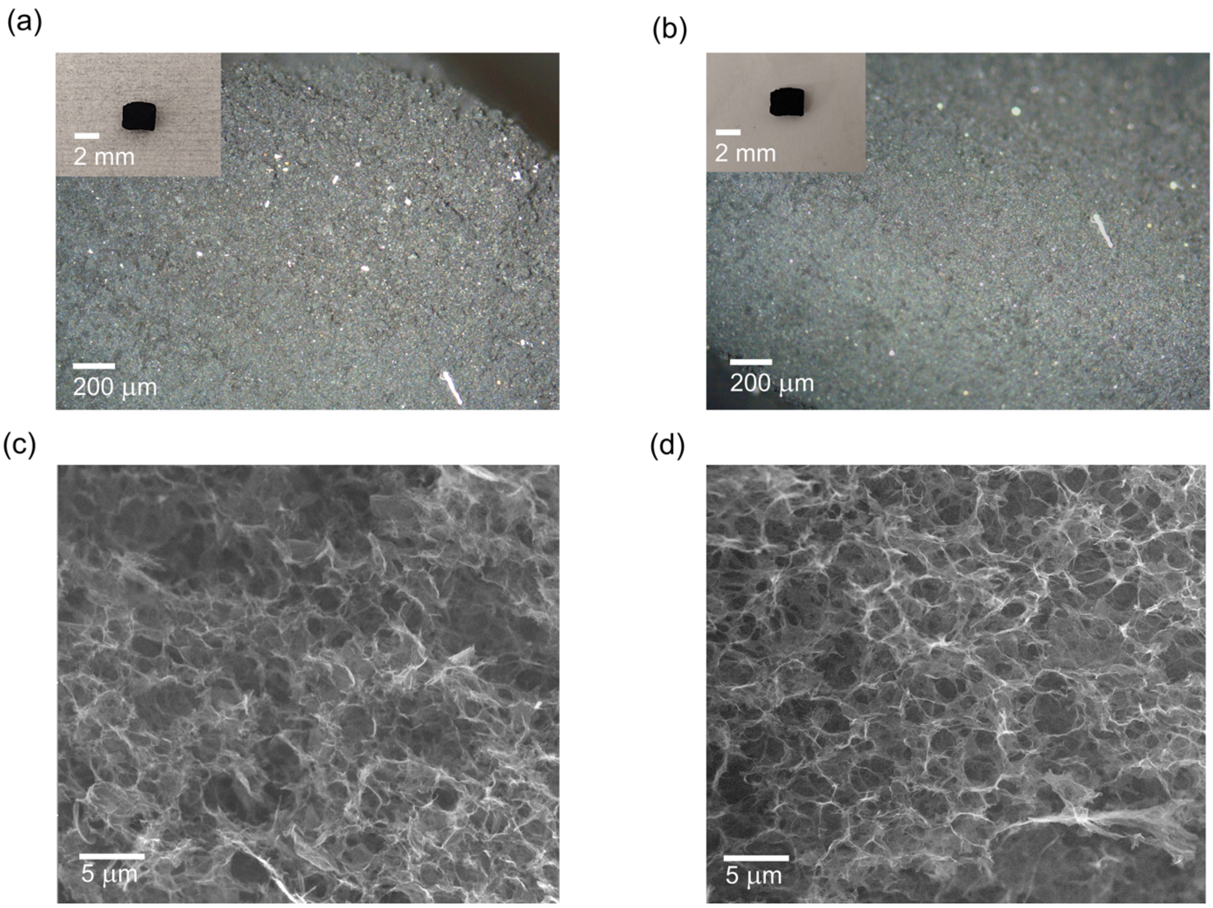

Figure S12: Optical and SEM images of a graphene aerogel sensing element (a,c) before and (b,d) after 5000 loading-unloading cycles.

Table S4: Comparison of our GA sensor with other reported strain-gauge sensors based on 3D graphene and other materials.

Materials	**Response**	**Gauge Factor (GF)/ Sensitivity (S, kPa^{-1}) (Strain Range)**	**Sensing Type**	**Response Time**	**Ref**
3D Graphene Aerogels	bilinear	GF_1 = 11.6 (0-8 kPa) GF_2 = 0.38 (8 kPa-1.18 MPa) S_1 = 53.5 MPa^{-1} (0-101 kPa) S_2 = 12.2 MPa^{-1} (101 kPa-1.18 MPa) GF_3 = 0.6 (0-0.3 MPa) GF_4 = 3.4 (0.3-0.55 MPa) S_3 = 0.39 MPa^{-1} (0-0.3 MPa) S_4 = 1.85 MPa^{-1} (0.3-0.55 MPa)	compression tension	0.52 ms (rise time) 0.61 ms (fall time)	**This work**
Graphene foam	linear	GF = 1.3	compression	-	1
Porous GO/rGO Hybrid film	nonlinear	S = 0.032 kPa^{-1}(0-1kPa)	compression	-	2
Graphene-Based Cellular Elastomers	linear	S_1 = 10 kPa^{-1} (0-200 Pa) S_2 = 0.23 kPa^{-1} (0-2.7 kPa)	compression	-	3
Graphene-amorphous carbon hierarchical foam	nonlinear	S = 11.47–5.19 kPa^{-1} (0-18 Pa)	compression	-	4
Biomimetic Architectured Graphene aerogels	nonlinear	S = 4 (50% strain)	compression	-	5
Graphene foam	bilinear	S = 22.8 ± 1.3 kPa^{-1} (0-10 Pa)	compression	-	6
Graphene aerogels	nonlinear	94% resistance change upon 60% compression	compression	250 ms (rise time) 150 ms (recovery time)	7
Sparkling graphene block	nonlinear	S_1 = 229.8 kPa^{-1} (0-0.1 kPa) S_2 = 26.7 kPa^{-1} (0.4-1 kPa)	compression	1,085 mm/s	8
Graphene sponge	bilinear	S_1 = 1.04 kPa^{-1} (13-260 Pa) S_2 = 0.12 kPa^{-1} (0.26-20 kPa)	compression	34 ms (response time) 5 ms (recovery time)	9
Graphene foam-like structure	bilinear	S_1 = 0.96 kPa^{-1} (<50 kPa) S_2 = 0.005 kPa^{-1} (>50 kPa)	compression	0.4–212 ms	10
Sponges coated with multiwalled carbon nanotubes and graphene	nonlinear	GF = 0.96–1.75	compression	< 750 ms	11
Graphene/silver nanowires sponge	linear	S_1 = 0.29 kPa−1 (0-2.5 kPa) S_2 = 0.02 kPa−1 (3-10 kPa) GF = 1.5 (0%–60% strain)	compression	54 ms	12
Graphene/polyurethane sponge	nonlinear	S = 0.75–3.08 kPa^{-1}	compression	14 ms	13

Graphene–Polyurethane Sponge	bilinear	S_1 = 0.26 kPa^{-1} (0–2 kPa) S_2 = 0.03 kPa^{-1} (2–10 kPa)	compression		[14]
3D periodic graphene aerogel microlattices	-	GF ~ 1 (50% strain)	compression	-	[15]
3D-printed graphene aerogel	linear	GF = 1.34 (up to 20% strain)	compression		[16]
Graphene foam/PDMS Porous Network Structure	bilinear	S = 0.09 kPa^{-1} (up to 2000 kPa) GF_1 = 2.6 (0−18%) GF_2 = 8.5 (22−40%)	compression	80–100 ms	[17]
Conventional metal alloys		Constantan wire: GF = 2.06 Constantan foil: GF = 2.04-2.16 NiCr. Foil: GF = 1.98-2.01			[18,19]

References

1 J. Kuang, L. Liu, Y. Gao, D. Zhou, Z. Chen, B. Han and Z. Zhang, *Nanoscale*, 2013, **5**, 12171.

2 S. Liu, X. Wu, D. Zhang, C. Guo, P. Wang, W. Hu, X. Li, X. Zhou, H. Xu, C. Luo, J. Zhang and J. Chu, *ACS Appl. Mater. Interfaces*, 2017, **9**, 24148–24154.

3 L. Qiu, M. Bulut Coskun, Y. Tang, J. Z. Liu, T. Alan, J. Ding, V.-T. Truong and D. Li, *Adv. Mater.*, 2016, **28**, 194–200.

4 Y. Ma, M. Yu, J. Liu, X. Li and S. Li, *ACS Appl. Mater. Interfaces*, 2017, **9**, 27127–27134.

5 M. Yang, N. Zhao, Y. Cui, W. Gao, Q. Zhao, C. Gao, H. Bai and T. Xie, *ACS Nano*, 2017, **11**, 6817–6824.

6 X. Zang, X. Wang, Z. Yang, X. Wang, R. Li, J. Chen, J. Ji and M. Xue, *Nanoscale*, 2017, **9**, 19346–19352.

7 K. Hu, T. Szkopek and M. Cerruti, *J. Mater. Chem. A*, 2017, **5**, 23123–23130.

8 L. Lv, P. Zhang, T. Xu and L. Qu, *ACS Appl. Mater. Interfaces*, 2017, **9**, 22885–22892.

9 S. Chun, A. Hong, Y. Choi, C. Ha and W. Park, *Nanoscale*, 2016, **8**, 9185–9192.

10 H. Tian, Y. Shu, X. F. Wang, M. A. Mohammad, Z. Bie, Q. Y. Xie, C. Li, W. T. Mi, Y. Yang and T. L. Ren, *Sci. Rep.*, 2015, **5**, 1–6.

11 Z. Ma, A. Wei, J. Ma, L. Shao, H. Jiang, D. Dong, Z. Ji, Q. Wang and S. Kang, *Nanoscale*, 2018, **10**, 7116–7126.

12 X. Dong, Y. Wei, S. Chen, Y. Lin, L. Liu and J. Li, *Compos. Sci. Technol.*, 2018, **155**, 108–116.

13 Y. Luo, Q. Xiao and B. Li, *RSC Adv.*, 2017, **7**, 34939–34944.

14 H.-B. Yao, J. Ge, C.-F. Wang, X. Wang, W. Hu, Z.-J. Zheng, Y. Ni and S.-H. Yu, *Adv. Mater.*, 2013, **25**, 6692–6698.

15 C. Zhu, T. Y.-J. Han, E. B. Duoss, A. M. Golobic, J. D. Kuntz, C. M. Spadaccini and M. A. Worsley, *Nat. Commun.*, 2015, **6**, 6962.

16 Q. Zhang, F. Zhang, S. P. Medarametla, H. Li, C. Zhou and D. Lin, *Small*, 2016, **12**, 1702–1708.

17 Y. Pang, H. Tian, L. Tao, Y. Li, X. Wang, N. Deng, Y. Yang and T.-L. Ren, *ACS Appl. Mater. Interfaces*, 2016, **8**, 26458–26462.

18 K. M. B. Jansen, *Exp. Mech.*, 1997, **37**, 245–249.

19 M.-H. Bao, in *Handbook of Sensors and Actuators*, 2000, pp. 199–239.